Evolutionary divergence of the necroptosis effector MLKL

Maria C. Tanzer[1,2], Indiana Matti[1,2], Joanne M. Hildebrand[1,2], Samuel N. Young[1], Ahmad Wardak[1], Anne Tripaydonis[1,2], Emma J. Petrie[1,2], Alison L. Mildenhall[1,2], David L. Vaux[1,2], James E. Vince[1,2], Peter E. Czabotar[1,2], John Silke[*,1,2,3], James M. Murphy[*,1,2,3]

[1]The Walter and Eliza Hall Institute of Medical Research, Parkville, Victoria 3052, Australia

[2]Department of Medical Biology, University of Melbourne, Parkville, Victoria 3050, Australia

[3] These authors share senior authorship

[*] To whom correspondence should be addressed:

jamesm@wehi.edu.au or silke@wehi.edu.au

Running title: Evolution of the necroptosis effector MLKL

Keywords: Programmed necrosis, gyrase, cell death, RIPK1, RIPK3, dimerization

Abbrevations: 4HB, 4-helix bundle; Cdc37, cell division cycle37; DMEM, Dulbecco's Modified Eagle's Medium; DOPS, 1,2-Dioleoyl-*sn*-glycero-3-phosphoserine; Dox, Doxycycline; FCS, Foetal Calf Serum; GST, Glutathione-S-transferase; HSP90, Heat Shock Protein90; MDF, Mouse Dermal Fibroblasts; MLKL, Mixed Lineage Kinase domain-Like; mMLKL, mouse MLKL; hMLKL, human MLKL; NTD, N-terminal domain; PIP, Phosphatidylinositol-phosphate; POPE, 1-Palmitoyl-2-oleoyl-*sn*-glycero-3-phosphoethanolamine; POPC, 1-Palmitoyl-2-oleoyl-*sn*-glycero-3-phosphocholine; POPG, 2-oleoyl-1-pamlitoyl-*sn*-glyecro-3-glycerol; Puro, Puromycin; RIPK, Receptor Interacting Protein Kinase; TLR, Toll-Like Receptor; TNF, Tumor Necrosis Factor; TSQ, TNF (T), Smac-mimetic Compound A (S), and QVD-OPh (Q);

ABSTRACT

The pseudokinase, MLKL (mixed lineage kinase domain-like), is the most terminal obligatory component of the necroptosis cell death pathway known. Phosphorylation of the MLKL pseudokinase domain by the protein kinase, Receptor Interacting Protein Kinase-3 (RIPK3), is known to be the key step in MLKL activation. This phosphorylation event is believed to trigger a molecular switch, leading to exposure of MLKL's N-terminal four-helix bundle (4HB) domain, its oligomerisation, membrane translocation, and ultimately cell death. To examine how well this process is evolutionarily conserved we analysed the function of MLKL orthologs. Surprisingly, and unlike their mouse, horse and frog counterparts, human, chicken and stickleback 4HB domains were unable to induce cell death when expressed in murine fibroblasts. Forced dimerisation of the human MLKL 4HB domain overcame this defect and triggered cell death in human and mouse cell lines. Furthermore, recombinant proteins from mouse, frog, human and chicken MLKL, all of which contained a 4HB domain, permeabilized liposomes, and were most effective on those designed to mimic plasma membrane composition. These studies demonstrate that the membrane permeabilization function of the 4HB domain is evolutionarily-conserved, but reveal that execution of necroptotic death by it relies on additional factors that are poorly conserved even amongst closely related species.

INTRODUCTION

Necroptosis is a form of programmed cell death that can be induced following ligation of death ligand and Toll-Like receptors (TLRs). Most experimental work has focused on necroptosis induced by Tumour Necrosis Factor (TNF). The key effectors in the pathway are the protein kinases, Receptor Interacting Protein Kinase (RIPK)-1 and RIPK3[1, 2, 3, 4], and the Mixed Lineage Kinase domain-Like (MLKL) pseudokinase[1, 5, 6, 7, 8]. RIPK3 phosphorylates the pseudokinase domain of MLKL, the most terminal known essential component of the pathway[5, 6], which is believed to induce a conformational change and unleash the N-terminal four-helix bundle (4HB) domain of MLKL: an executioner domain[5, 9, 10]. Several models have been proposed for how this 4HB domain might induce cell death, including activation of downstream effectors, such as ion channels[11, 12], direct permeabilisation of membranes and/or formation of a transmembrane pore[13, 14], all of which remain the subject of debate. The consensus from these and other studies is that in order to kill, MLKL must translocate to membranes and assemble into high molecular weight signalling complexes, which are likely to be MLKL oligomers, although the stoichiometry of these MLKL oligomers remains an open question[10, 11, 12, 13, 14]. Nonetheless, phosphorylation appears to be a key cue for MLKL activation[15] and, as the most terminal known post-translational modification in the pathway, could potentially be utilised as a biomarker in pathologies arising from necroptotic cell death[14, 16].

A model whereby RIPK3-mediated phosphorylation of the MLKL pseudokinase domain activation loop (S345 in mouse; T357/S358 in human) leads to unleashing of the executioner 4HB domain is supported by several lines of evidence. Firstly, expression of the isolated mouse MLKL 4HB or the complete N-terminal domain (NTD) killed mouse dermal fibroblasts[10]. Secondly, cell death occurred to a similar extent when full length mouse MLKL

harbouring the S345D mutation, that mimics activation loop phosphorylation by RIPK3, was expressed in murine fibroblasts[5, 15, 17]. Additionally, three studies have attributed a direct membrane-permeabilization function to recombinant human MLKL 4HB domain in *in vitro* liposome dye-release assays[13, 14, 18]. However, a number of questions remain unanswered. It is unclear why S345D mouse MLKL is a potent killer of murine fibroblasts, while the human counterpart, T357D/S358E, induced death of HT29 cells in one study[19], yet did not induce pronounced death of human U2OS cells unless dimerised via a fused domain[14]. Similarly, it is unclear why forced dimerisation of mouse MLKL 4HB domain was required for cell death in L929, CHO and HeLa cells[12], but not in MDFs[10]. It is also unclear why recombinant human MLKL 4HB domain exhibits a preference for substrate liposomes containing cardiolipin, high concentrations of which are considered to be confined to mitochondrial inner membranes[14, 18], even though mitochondria are dispensable for necroptotic death[20]. Additionally, the human MLKL 4HB domain potently and rapidly induced membrane permeabilisation in liposome assays[13, 14, 18], yet a substantial delay in cell death is observed following MLKL membrane translocation[15]. These observations led us to investigate the differential susceptibility of different cell types to MLKL induced necroptotic death and whether reduced susceptibility could be overcome by inducible dimerisation of either full length MLKL or the 4HB domain, Finally we determined the extent to which the necroptotic inducing properties are conserved between MLKL orthologs.

We found that the human MLKL NTD, and 4HB domain encoded within, did not cause death of the commonly studied human cell lines, U937, HT29 and HeLa. However, inducible dimerisation of the human MLKL 4HB domain via a fused gyrase domain led to robust killing of these cell lines as well as wild-type, but not *Mlkl*$^{-/-}$ MDFs. Analogously, dimerisation of full-length wild-type mouse MLKL via a fused gyrase domain led to death of

wild-type and *Mlkl*$^{-/-}$ MDFs in the absence of necroptotic stimuli. Interestingly, NTDs from mouse, horse and frog MLKL, but not human, chicken and stickleback MLKL, induced death of *Mlkl*$^{-/-}$ MDFs. Nonetheless, using liposome permeabilization assays, we demonstrated that like the mouse and frog MLKL NTDs, human and chicken MLKL NTDs compromised membrane integrity, and were more effective on liposomes whose composition resembled that of plasma membranes than on those mimicking mitochondrial membranes. Collectively, these studies demonstrate that although the MLKL 4HB domain encodes an evolutionarily-conserved membrane permeabilisation function, execution of necroptotic death relies on the presence or absence of endogenous factors that are not universally expressed in U937, HT29, HeLa and MDF cells to either mediate MLKL oligomerisation, membrane translocation and/or downstream signalling.

RESULTS

Cell death induction by the NTD of human MLKL requires dimerisation

Our earlier work demonstrated that expression of the N-terminal domain (NTD) of mouse MLKL (mMLKL; residues 1-180) or the mMLKL four-helix bundle (4HB) domain (residues 1-125) killed mouse fibroblasts in the absence of a conventional necroptotic stimulus such as TSQ: TNF (T), Smac-mimetic (S), and Q-VD-OPh (Q)[10]. In contrast, in the present work we observed that expression of the analogous human MLKL (hMLKL) NTD (residues 1-180) in U937, HT29 and HeLa cells did not induce stimulus-independent cell death (Figure 1A-C).

Our earlier studies demonstrated that mMLKL(1-180) spontaneously assembled into a high molecular weight complex in membranes[10]. The lack of killing by hMLKL(1-180) led us to determine whether the human domain lacked an intrinsic capacity to oligomerise. We tested this hypothesis by fusing *E. coli* DNA gyrase (Figure 1D, E), a domain that can be dimerised by the divalent antibiotic coumermycin, to the C-termini of hMLKL(1-180; NTD) and hMLKL(1-125; 4HB) domains[21]. In the absence of coumermycin, the fusion proteins behaved the same as the unfused domains in the absence of apoptotic (TS) or necroptotic (TSQ) stimuli (*cf*. Figure 1A and Figure 1F, G). Similarly, a C-terminally StrepII tagged version of hMLKL(1-125) did not induce stimulus-independent cell death (Supplementary Figure 1A-C). However, addition of coumermycin to cells expressing either of these domains led to their death without requiring other stimuli (Figure 1F, G), suggesting that the hMLKL NTD was simply less effective at oligomerising than its murine counterpart. Notably, the observed cell death confirms that fusion to gyrase did not compromise NTD folding or stability, nor impose a dimer configuration that is incompatible with induction of necroptosis. To test this more rigorously, we expressed the constructs in HT29 cells (Figure 1H, I). Unexpectedly, even though hMLKL(1-180) gyrase was well expressed (Supplementary Figure 1F), coumermycin-

induced dimerisation did not induce stimulus-independent cell death in HT29 cells (Figure 1H). It is possible that the lack of HT29 death at 48 h is reflective of the generally slower necroptosis kinetics in HT29s, as observed upon TSQ stimulation. However, expression of the hMLKL 4HB domain (1-125) in HT29 cells induced cell death in the absence of coumermycin, and addition of coumermycin increased cell death (Figure 1I), at 48 hours. In HeLa cells, coumermycin-mediated dimerisation of hMLKL(1-180) and (1-125) gyrase fusions was required to induce death (Figure 1J, K), with more death observed for hMLKL(1-125) than hMLKL(1-180). These findings are consistent with the idea that oligomerisation is not an intrinsic property of the hNTD but requires additional factors that are not present in all cells. Furthermore, these data support the notion that the amino acids from 125-180 can inhibit the killing function of the hMLKL 4HB domain.

Human and mouse MLKL NTDs and activated mutant constructs are poor killers of cells of the opposite species

While expression of mMLKL(1-180) or the 4HB domain (1-125) potently kills wild-type and *Mlkl*-deficient mouse dermal fibroblasts (MDFs)[10], the capacity of human constructs to kill these murine cells has not yet been examined. We therefore expressed the hMLKL(1-180) gyrase fusion in wild-type and *Mlkl*$^{-/-}$ MDFs, and observed no cell death either in the absence or presence of dimerisation by coumermycin (Figure 2A, B). In contrast, forced dimerisation of the hMLKL(1-125) gyrase fusion caused wild-type, but not *Mlkl*$^{-/-}$, MDFs to die (Figure 2C, D). These data suggest that the hMLKL 4HB domain cannot induce death in MDFs independently, but can augment the activity of endogenous mouse MLKL when dimerised.

To preclude the possibility that the absence of the pseudokinase domain from these expression constructs might compromise their killing functions, we attempted to reconstitute

necroptosis signalling in *Mlkl*$^{-/-}$ MDFs with constructs encoding full-length (FL) mouse and human MLKL (Figure 2E, Supplementary Figure 2A). As observed previously[5], mMLKL reconstituted the necroptosis pathway (Supplementary Figure 2A), however, consistent with an earlier report[22], human MLKL did not (Figure 2E), despite evident expression (Supplementary Figure 2B). Taken together, these data demonstrate evolutionary divergence in the intrinsic capabilities of MLKL 4HB domains to induce cell death, and the evolution of species-specific necroptosis mechanisms in which MLKL orthologs do not readily complement one another.

Full length mouse MLKL (residues 1-464) bearing the S345D mutation that mimics activation by RIPK3-mediated phosphorylation, is a potent killer of mouse fibroblasts in the absence of stimuli[5, 15, 17]. To determine whether a deficit in endogenous mouse RIPK3-mediated activation of hMLKL underpins the inability of hMLKL to reconstitute mouse fibroblasts, we tested whether full length hMLKL bearing the phosphomimetic mutations, T357E/S358E (TSEE), was lethal to wild-type or *Mlkl*$^{-/-}$ MDFs (Figure 2F). Unlike the S345D mMLKL mutant[5, 15, 17], the hMLKL TSEE mutant did not induce death of either wild type or *Mlkl*$^{-/-}$ MDFs (Figure 2F). Similarly, expression of the hMLKL TSEE mutant in the human cell lines, U937 and HT29, did not induce cell death (Figure 2G, H). More surprisingly, expression of this mutant construct inhibited TSQ induced necroptosis in U937 cells (Figure 2G), suggesting a dominant negative activity. Because mMLKL(1-464) bearing the S345D mutation is a potent death effector in mouse fibroblasts[5, 15, 17], we next asked whether it induced cell death in human cell lines. However, neither S345D mMLKL(1-464) nor mMLKL(1-180) were able to induce death of HT29 cells (Figure 2I, J), despite both being potent killers of mouse fibroblasts[5, 10, 15, 17]. In contrast, expression of S345D mMLKL(1-464) in U937 cells led to a modest, but reproducible, amount of death (Figure 2K). The killing

activity of S345D mMLKL(1-464) corresponded with its capacity to translocate from the cytoplasmic (C) fraction to membranes (M) and assemble into a high molecular weight species (Figure 2L). In contrast, hMLKL(1-180) did not undergo oligomerisation or membrane translocation in parallel experiments (Figure 2L), in keeping with its inability to induce death of U937 cells. Collectively, these data support the idea that cell-specific factors determine whether mouse or human MLKL NTD or activated mutant constructs are able to kill, and whether dimerisation mediated by a fused domain can, at least in part, overcome a requirement for these factors.

Dimerisation of full length MLKL drives cell death

Consistent with the hypothesis that MLKL must be activated by RIPK3 phosphorylation, ectopic expression of mMLKL alone does not induce necroptosis[5, 10, 15]. Whilst expression of activating mutants can overcome the requirement for RIPK3 phosphorylation[5, 15], it has not been established whether forced dimerisation of mMLKL can similarly cause death in the absence of stimuli. We examined this by fusing full-length mMLKL to a gyrase domain (Figure 3A) and expressing in wild-type and *Mlkl*$^{-/-}$ MDFs (Figure 3C, D). Stimulus-independent death was only observed upon coumermycin-mediated dimerisation in wild-type and *Mlkl*$^{-/-}$ MDFs (Figure 3C, D), confirming the importance of oligomerisation in MLKL activation as a likely prerequisite for membrane translocation. We explored this hypothesis by characterising two loss-of-function mouse MLKL 4HB domain point mutants, R105A/D106A and E109A/E110A, that we have shown fail to translocate to membranes and assemble into high molecular weight complexes[10] (Figure 3B). As expected from our earlier studies with the untagged versions[10], these mMLKL-gyrase mutants failed to reconstitute TSQ-mediated necroptosis when expressed in *Mlkl*$^{-/-}$ MDFs (ref.[10] and Figure 3F, H). Interestingly, however, they did not induce death even when dimerisation was forced by coumermycin, either in wild

type (Figure 3E, G) or *Mlkl*$^{-/-}$ MDFs (Figure 3F, H). The inability of dimerisation to rescue the killer function of these mutants suggests that the Ala substitutions compromise higher order oligomerisation or interactions with other proteins that are crucial for MLKL-mediated cell death.

We used an analogous approach to examine whether forced dimerisation of wild-type or the phosphomimetic T357E/S358E (TSEE) human MLKL could induce death of wild-type or *Mlkl*$^{-/-}$ MDF, U937, HT29 and HeLa cells (Figure 4). Interestingly, death of wild-type MDF, HT29 and HeLa cells only occurred following forced dimerisation via the fused gyrase domain and, surprisingly, to the same extent for wild-type and phosphomimetic mutant. As observed for TSEE hMLKL expression in U937 (Figure 2G), dimerised TSEE hMLKL suppressed endogenous necroptosis signalling upon TSQ stimulation (Figure 4F), whereas wild-type hMLKL did not (Figure 4E).

The NTDs of mouse, horse & frog, but not human, chicken & fish, MLKL orthologs kill mouse cells

Our observations that the human MLKL NTD did not kill mouse fibroblasts, and mMLKL(1-180) did not kill human HT29 cells (Figure 2), led us to test the killing capacities of MLKL 4HB domains from other species (Figure 5A). We therefore expressed the NTD of mouse, human, horse, frog, chicken and stickleback MLKL, all bearing C-terminal StrepII tags to allow expression to be monitored by Western blot (Supplementary Figure 2C-H), in *Mlkl*$^{-/-}$ MDFs, and evaluated their intrinsic cell killing capacities (Figure 5B-G). Expression of mouse, horse and frog MLKL NTD induced death of *Mlkl*$^{-/-}$ MDFs (Figure 5D, E), while the human, chicken and stickleback counterparts did not (Figure 5C, F, G). Using the capacity of the 3H1 anti-MLKL antibody to detect mouse and horse MLKL NTD, we observed that horse MLKL(1-189) translocated to membranes and assembled into high molecular weight

complexes by Blue-Native PAGE, two hallmarks of MLKL activation, as observed for mMLKL(1-180) (Figure 5H and ref.[10]). These data suggest a common mechanism of action between mouse and horse MLKL NTDs in inducing cell death.

Recombinant MLKL NTDs permeabilise liposomes with compositions resembling those of plasma membranes

While the foregoing results are consistent with the hypothesis that there are cell specific factors required for the NTDs to kill cells (summarized in Figure 6A and Supplementary Figure 3), an alternative explanation is that deficits in cell death induction among MLKL orthologs arise from an intrinsic inability to permeabilise membranes. To test this, we prepared recombinant mouse, human, chicken and frog MLKL proteins (Figure 6B), and tested their ability to directly permeabilise liposomes mimicking plasma or mitochondrial membrane compositions *in vitro* (Figure 6C-K). Unfortunately, we were unable to express and purify recombinant frog NTD. Each of the NTD and full-length MLKL proteins were more effective in permeabilising liposomes with plasma membrane-like composition than those of resembling mitochondrial membranes (Figure 6C-K). This preference was most apparent among the NTDs of mouse and chicken MLKL (Figure 6C, D). Among the NTD constructs, hMLKL(2-154) (Figure 6E) was a poorer mediator of membrane permeabilisation than either mMLKL(1-169) or chicken MLKL(2-156) (Figure 6C, D). Full length MLKL proteins were more potent membrane disruptors than their NTDs, raising the possibility that the pseudokinase domain may facilitate either stabilisation of the NTD or organisation of MLKL monomers into higher order, membrane permeabilising assemblies. Importantly, we detected only negligible liposome permeabilisation in control experiments using recombinant pseudokinase domains (Figure 6I-K), in keeping with a role for the NTDs within the full-length MLKL proteins in mediating membrane perforation. These results indicate that the

NTD of MLKL encodes an intrinsic, evolutionarily conserved capacity to permeabilise plasma membranes.

DISCUSSION

MLKL contains a C-terminal pseudokinase domain that, until phosphorylated by RIPK3 in its activation loop, suppresses the executioner function of the N-terminal four-helix bundle (4HB) domain. Several studies have implicated the N-terminal domain (NTD), which encompasses the 4HB domain, as the mediator of cell death[10, 11, 12, 13]. These studies suggest the simple hypothesis that RIPK3 phosphorylates MLKL leading to a conformational change, exposure of the NTD, resulting in MLKL membrane localisation, oligomerisation and membrane permeabilisation. However, a more complicated mechanism is suggested by studies in L929, CHO and HeLa cells, where dimerisation via a fused domain was necessary for the NTD of mouse MLKL to induce cell death[12].

Taken together, these studies led us to hypothesize that cell type-specific factors, such as proteins that modulate MLKL activation and 4HB domain exposure, oligomerisation, membrane translocation and permeabilization are necessary for MLKL 4HB domain induced cell death (summarized in Figure 6A). The identities of these proteins (termed X1-X4 in Figure 6A) are of enormous interest to the field and we have recently identified one such factor, the co-chaperone system Cdc37-HSP90, as an important mediator of MLKL activation[23], which can be considered as putative X1 proteins. In addition, we have shown that phosphorylation of the MLKL activation loop coincides with MLKL oligomerisation and membrane translocation but that these events precede membrane permeabilisation by several hours[15], again strongly implying that this is a regulated, rate limiting, stage in MLKL killing and imply the existence of X4 factors. We also recently described sites of MLKL

phosphorylation outside of the activation loop that can positively and negatively regulate necroptosis signalling[15]. These findings suggest that putative X1 proteins may post-translationally modify MLKL and thereby determine the threshold for MLKL induced cell death[15, 24, 25].

A key step in MLKL activation is its oligomerisation (Figure 6A; Supplementary Figure 3). While this is readily accomplished by mMLKL NTD or 4HB domains expressed in MDFs, forced dimerisation of their human counterparts was required to kill human cells. Notably, hNTD dimerisation could only measurably kill U937 cells, while h4HB domain dimerisation killed wild-type MDF, U937, HT29 and HeLa cells, suggesting that in some cell types the brace helix encodes an inhibitory function, possibly preventing oligomerisation, consistent with previous findings[13, 18]. Furthermore these data imply that there are cell specific factors that are required to enable hMLKL to translocate to membranes, oligomerise and permeabilise membranes.

Recently, we established that hMLKL phosphorylation led to immediate membrane translocation and assembly of phospho-MLKL into higher order complexes, with cell death following some hours later[15]. To further test the simple hypothesis that phosphorylation by RIPK3 induces a conformational change in MLKL leading to exposure of the NTD, we examined whether full-length MLKL constructs bearing mutations that mimicked RIPK3-mediated phosphorylation, T357E/S358E (TSEE) hMLKL and S345D mMLKL, could induce death in MDFs, U937 and HT29 cells. Consistent with our hNTD results, TSEE hMLKL did not induce death in wild-type or *Mlkl*$^{-/-}$ MDFs, HT29 or U937 cells, whereas the murine S345D MLKL mutant caused death of U937 cells. Thus the phosphorylation equals activation hypothesis is too simplistic. Expression of a related T357E/S358D hMLKL construct in

U2OS or HT29 cells was previously reported to induce ~30% cell death[14, 19], which was enhanced to ~50% in U2OS cells via dimerisation of a fused domain[14]. In contrast, using our expression system, we only observed measurable death of wild-type MDF, HT29 or HeLa cells following forced dimerisation of wild-type or T357E/S358E hMLKL via a fused gyrase domain, and the extent of death was comparable for wild-type and phosphomimetic mutant constructs. Taken together these studies imply that killing by hMLKL requires activating signals or interactions in addition to RIPK3 phosphorylation, possibly by promoting MLKL oligomerization.

To further understand the unexpected species-specific difference in the ability of human and mouse MLKL NTDs to kill cells we examined whether the NTDs of MLKL orthologs could induce cell death. In contrast to the human, chicken and stickleback MLKL NTDs, the mouse, horse and frog MLKL orthologs induced cell death. By comparing amino acid sequences, we identified the α4 helix residues that align with mouse R105 and E109 as conserved basic and acidic residues, respectively, among mouse, horse and frog MLKL NTDs, but divergent among the non-killing human, chicken and stickleback MLKL. The importance of these residues for cell death was previously inferred from our earlier alanine scanning mutagenesis studies of the mMLKL 4HB domain, where R105A/D106A and E109A/E110A were loss of function mutants that had lost the capacity to translocate to membranes and assemble into high molecular complexes[10]. Here, we showed that wild-type mMLKL dimerised via a fused gyrase domain can induce cell death in wild-type and *Mlkl*$^{-/-}$ MDFs, whilst forced dimerization of constructs harbouring the R105A/D106A or E109A/E110A mutations could not. These data indicate that the earlier reported defective membrane translocation by these mutants[10] cannot be rescued by forced oligomerisation, consistent with an essential role for these residues in either assembly of higher order MLKL oligomers, membrane translocation

or recruitment of downstream factors required for induction of necroptosis rather than MLKL activation *per se*.

Previous studies have demonstrated that the hMLKL 4HB domain possesses an intrinsic capacity to permeabilise membranes in *in vitro* liposome assays[13, 14, 18], however it remained unclear whether this is a broadly conserved function among orthologs and, if so, why all MLKL 4HB domains do not induce death upon expression in cells. Earlier work established a preference of hMLKL 4HB domain for permeabilising liposomes with 15% cardiolipin or high PIP_2 compositions[13, 14]. The relevance of the former is unclear because cardiolipin is believed to be exclusively mitochondrially-localised, yet mitochondria and the PGAM5-Drp1 mitochondrial fragmentation pathway are not universally required for necroptosis[5, 20, 26, 27, 28]. Here, we observed that the 4HB domains of mouse and frog MLKL, which kill MDFs, and human and chicken 4HB domains, which do not, exhibited a clear preference for plasma membrane over mitochondrial composition liposomes. Unexpectedly, full length human, frog and chicken MLKL were more potent and rapid inducers of membrane permeabilisation than the recombinant NTDs alone, suggesting a function for the pseudokinase domain in augmenting 4HB domain-mediated membrane permeabilisation. While an intrinsic membrane permeabilisation function is clearly conserved between orthologous 4HB domains, no RIPK3 orthologs have been identified in frog, chicken and stickleback, suggesting that other kinases are likely to have evolved compensatory roles as modulators of MLKL activation. Considered together with the cellular studies, our data argue for the existence of additional factors in cells that either suppress MLKL mediated killing (which might be absent in MDFs) or are required for MLKL to induce necroptosis, for example by promoting its oligomerisation. How the conserved membrane permeabilisation function of the MLKL 4HB domain is regulated within cells remains of enormous interest and highlights the importance of identifying additional

effectors within these cells, which either serve to augment MLKL-driven necroptosis or to suppress the membrane permeabilisation function of the 4HB domain.

MATERIALS AND METHODS

Expression constructs

Synthetic cDNAs encoding mouse (*Mus musculus*; residues 1-464) and human (*Homo sapiens*; residues 1-471) MLKL were synthesized by DNA2.0, CA, cDNAs encoding chicken (*Gallus gallus*; residues 1-486), frog (*Xenopus laevis*; residues 1-498), horse (*Equus caballus*; residues 1-189, N-terminal domain only) MLKL were synthesised by Bioneer (South Korea) and stickleback MLKL (*Gasterosteus aculeatus*; residues 1-471) was synthesised by GeneArt (Germany). All oligonucleotides for PCR amplifications and oligonucleotide-directed mutagenesis were synthesised by IDT (Singapore or Coralville, IA). For expression in mammalian cell lines, cDNAs were ligated into the doxycycline-inducible puromycin-resistant lentiviral vector, pFTRE3G PGK Puro[5, 10], or cDNAs lacking a stop codon were ligated in-frame as BamHI-NheI fragments into derivative vectors encoding either a C-terminal StrepII tag for detection of expression[15] or *E. coli* DNA GyraseB domain for oligomerisation studies[21]. For expression of recombinant proteins, cDNAs encoding human MLKL (2-154) was ligated in-frame C-terminal to a TEV protease-cleavable GST tag in the vector pGEX-2T-TEV, and chicken MLKL (2-156) was ligated in-frame C-terminal to a NusA-His_6 tag in pETNusH Htb, as described for mouse MLKL (1-169) previously[10]. Full-length human (2-471), chicken (2-486) and frog (2-498) MLKL and frog (195-498) pseudokinase domains were expressed from insect cells as described previously for mouse MLKL [5, 10] using the Bac-to-Bac system (LifeTechnologies), but with a TEV-cleavable N-terminal GST tag for expression of human (2-471) and frog (2-498) MLKL rather than an N-terminal His_6 tag. Human MLKL pseudokinase domain (190-471) was expressed and purified

as before[29]. The sequences of all DNA inserts were verified by Sanger sequencing (Micromon Facility, VIC), and are available on request.

Cell lines and cell death assays

U937 and HT29 cells were cultured in human tonicity RPMI medium and HeLa cells in Dulbecco's modified Eagle's medium (DMEM) both supplemented with 8-10% v/v fetal calf serum (FCS) and puromycin (5 μg/mL) for lines stably transduced with MLKL expression constructs. Cell death assays were carried out in 48 well plates, seeded at 1.5 x 10^4 for HT29 and 3 x 10^4 for U937 and HeLa cells per well, as described previously[15]. Cells were left for 48 h and treated for 4 hours with 10 ng/mL doxycycline and coumermycin (700 nM) when gyrase fusions were expressed. Cells were either left untreated or treated with TNF (100 ng/mL) and the Smac-mimetic, Compound A (500 nM), or TNF, Compound A and the pan-Caspase inhibitor, Q-VD-OPh (10 μM), after 24 h or 48 h harvested as described in the figure legends, stained with propidium iodide (PI; 1 μg/mL) and quantitated by flow cytometry.

Three independent lines of *Mlkl*$^{-/-}$ and wild-type mouse dermal fibroblasts (MDFs) were generated as described previously[30]. MDFs and HEK293T were maintained in DMEM supplemented with 8-10 % v/v FCS, and puromycin (2 μg/mL) for lines stably transduced with MLKL expression constructs. Cell death assays were carried out in 24 well plates, seeded at 5 x 10^4 cells per well, as before[15]. Cells attached overnight and then induced for 4 hours with 10 ng/mL doxycycline and then left either untreated or treated with TNF and Smac mimetic, or the TNF, Smac-mimetic and Q-VD-OPh cocktail, as above. Quantitation of cell death by flow cytometry was performed 24 hours post-stimulation.

Statistical analyses

Error bars represent Mean ± SEM of specified number of independent and/or biological repeats of cell death assays, not technical replicates. Liposome permeabilisation assays are presented as the Mean ± SD of independent experiments.

Fractionation and Blue Native PAGE

Fractionation of cells into cytoplasmic and membrane fractions was performed as described previously[10, 15]. Briefly, U937 or MDF cells stably transduced with mutant MLKL constructs were induced as indicated in the figure legends, before cells were harvested and permeabilized in buffer (20 mM HEPES pH 7.5, 100 mM KCl, 2.5 mM $MgCl_2$, and 100 mM sucrose) containing 0.025% digitonin (BIOSYNTH, Staad, Switzerland), 2 μM N-ethyl maleimide, phosphatase and protease inhibitors. Crude membrane and cytoplasmic fractions were separated by centrifugation (5 min at 11000 g), and the respective fractions prepared in buffers to a final concentration of 1% w/v digitonin. Samples were resolved on a 4-16% Bis-Tris Native PAGE gel, transferred to PVDF for Western blot analyses.

Western blot antibodies

Antibodies used for Western blotting were: the rat anti-MLKL 3H1 monoclonal (produced in-house[5]; available as MABC604, EMD Millipore), which detected mouse, human and horse MLKL; anti-Strep-tag II (ab76949, Abcam); StrepTactin-HRP (2-1502-001, IBA); rabbit anti VDAC1 (AB10527, Millipore); rabbit anti GAPDH (2118, Cell Signalling Technology); mouse anti Actin (A-1987, Sigma).

Recombinant protein production

Pseudokinase domains from mouse (179-464) and frog (195-498) MLKL, full length frog (2-498) and chicken (2-486) MLKL were expressed and purified from Sf21 insect cells, as

described for full length mouse MLKL and its pseudokinase domain previously[5, 10, 15], albeit with a TEV protease cleavable N-terminal GST tag for frog MLKL (2-498) instead of the N-terminal His_6 used otherwise. Mouse MLKL N-terminal domain (1-169) was expressed fused to an N-terminal NusA-His_6 tag and purified from *E. coli* BL21 Codon Plus as previously[10]. Chicken MLKL (2-156) was prepared analogously. The N-terminal domain of human MLKL (2-154) was expressed in *E. coli* BL21 Codon Plus fused to an N-terminal GST tag encoded by the vector, pGEX-2T-TEV. Purification was performed using standard protocols[21, 31]. Briefly, 0.6L Super broth cultures containing 100 μg/mL ampicillin were inoculated with transformed *E. coli* and cultured at 37°C with shaking to OD_{600} of 0.6-0.8. Cultures were then cooled to 18°C, protein expression induced by addition of 1mM IPTG with continued shaking and incubation at 18°C overnight. Cell pellets were resuspended in lysis buffer (200mM NaCl, 20mM HEPES pH 7.5, 0.5mM TCEP) supplemented with 2mM PMSF, before lysis by sonication, elimination of debris by centrifugation at 45000 g, 0.45μm filtration of the lysate and incubation with glutathione agarose (UBP Bio) at 4°C with agitation for 1-2 h. Beads were collected and washed extensively with lysis buffer before incubation with 200μg TEV protease at 20°C for 2h. Supernatant containing cleaved MLKL N-terminal domain was concentrated by centrifugal ultrafiltration and loaded on to Superdex S200 gel filtration column pre-equilibrated with gel filtration buffer (200mM NaCl, 20mM HEPES pH 7.5). Fractions containing purified MLKL N-terminal domain as assessed by SDS-PAGE were pooled, concentrated by centrifugal ultrafiltration to 5-10mg/mL, snap frozen as 50 μL aliquots in liquid nitrogen and stored at -80°C until required. All recombinant proteins used in liposome studies were eluted from Superdex-200 in gel filtration buffer.

Liposome permeabilisation assays

Liposomes of plasma membrane (20% POPE, 40% POPC, 10% phosphoinositol, 20% DOPS, 10% POPG; based on references[32, 33]) and mitochondrial (30% POPE, 45% POPC, 10% phosphoinositol, 15% cardiolipin; based on ref.[18]) mimetic compositions were assembled from lipids purchased from Avanti Polar Lipids and resuspended in chloroform at 20 mg/mL. Lipids were mixed to a final volume of 100 µL, solvent was evaporated under N_2 gas followed by vacuum. 18.8 mg of 5(6)-carboxyfluorescein was solubilized in 100 µL of 1 M NaOH, spun at 14000 g for 1 min, before 25 µL of 1 M HEPES pH 7.5 added and the volume made up to 1 mL with milliQ water to a final concentration of 50mM. Dried lipids were resuspended in 1 mL 50 mM 5(6)-carboxyfluorescein solution, vortexed and sonicated, then liposomes extruded through a 100 nm pore membrane. Liposomes were purified from excess 5(6)-carboxyfluorescein by gel filtration using PD10 columns (GE Healthcare) equilibrated in SUV buffer (10 mM HEPES pH 7.5, 135 mM KCl, 1 mM $MgCl_2$) and eluted in 2.5mL SUV buffer to yield liposomes at 30 µM concentration. Liposomes (10 µM) were incubated with 1 µM recombinant protein at 20°C with dye release monitored spectrophotometrically (excitation 485nm, emission 535 nm) starting 15min after components were assembled, and collecting every subsequent 30min for a further 3 hours. 100% dye release was determined in parallel by incubation of liposomes with 1% Triton-X100.

ACKNOWLEDGMENTS

We thank Professor Mark Hampton and Dr Andreas Konigstorfer for kindly providing HT29 cells and Dr Toru Okamoto for development of the inducible lentiviral vector. This work was supported by National Health and Medical Research Council of Australia (NHMRC) grants (461221, 1046010, 1051210, 1057888, 1057905, 1067289) and fellowships to JMH (541951), DLV (1020136), JEV (1052598), PEC (1079700) and JS (541901, 1058190); an Australian Research Council Future Fellowship to JMM (FT100100100); a Victorian International Research Scholarship to MCT; with additional support from the Victorian State Government Operational Infrastructure Support and NHMRC IRIISS grant (9000220).

CONFLICTS OF INTEREST

JS is a member of the Scientific Advisory Board of TetraLogic Pharmaceuticals Corporation. JMM co-leads a program funded by Catalyst Therapeutics Pty Ltd and the Walter and Eliza Hall Institute to develop necroptosis inhibitors. The other authors declare no conflict of interest.

REFERENCES

1. Cho YS, Challa S, Moquin D, Genga R, Ray TD, Guildford M*, et al.* Phosphorylation-driven assembly of the RIP1-RIP3 complex regulates programmed necrosis and virus-induced inflammation. *Cell* 2009, **137**(6)**:** 1112-1123.

2. He S, Wang L, Miao L, Wang T, Du F, Zhao L*, et al.* Receptor interacting protein kinase-3 determines cellular necrotic response to TNF-alpha. *Cell* 2009, **137**(6)**:** 1100-1111.

3. Holler N, Zaru R, Micheau O, Thome M, Attinger A, Valitutti S*, et al.* Fas triggers an alternative, caspase-8-independent cell death pathway using the kinase RIP as effector molecule. *Nat Immunol* 2000, **1**(6)**:** 489-495.

4. Degterev A, Hitomi J, Germscheid M, Ch'en IL, Korkina O, Teng X*, et al.* Identification of RIP1 kinase as a specific cellular target of necrostatins. *Nat Chem Biol* 2008, **4**(5)**:** 313-321.

5. Murphy JM, Czabotar PE, Hildebrand JM, Lucet IS, Zhang JG, Alvarez-Diaz S*, et al.* The pseudokinase MLKL mediates necroptosis via a molecular switch mechanism. *Immunity* 2013, **39**(3)**:** 443-453.

6. Sun L, Wang H, Wang Z, He S, Chen S, Liao D*, et al.* Mixed lineage kinase domain-like protein mediates necrosis signaling downstream of RIP3 kinase. *Cell* 2012, **148**(1-2)**:** 213-227.

7. Zhao J, Jitkaew S, Cai Z, Choksi S, Li Q, Luo J*, et al.* Mixed lineage kinase domain-like is a key receptor interacting protein 3 downstream component of TNF-induced necrosis. *Proceedings of the National Academy of Sciences of the United States of America* 2012, **109**(14)**:** 5322-5327.

8. Wu J, Huang Z, Ren J, Zhang Z, He P, Li Y*, et al.* Mlkl knockout mice demonstrate the indispensable role of Mlkl in necroptosis. *Cell research* 2013, **23**(8)**:** 994-1006.

9. Czabotar PE, Murphy JM. A tale of two domains - a structural perspective of the pseudokinase, MLKL. *FEBS J* 2015, **In press**(doi: 10.1111/febs.13504).

10. Hildebrand JM, Tanzer MC, Lucet IS, Young SN, Spall SK, Sharma P*, et al.* Activation of the pseudokinase MLKL unleashes the four-helix bundle domain to induce membrane localization and necroptotic cell death. *Proceedings of the National Academy of Sciences of the United States of America* 2014, **111**(42)**:** 15072-15077.

11. Cai Z, Jitkaew S, Zhao J, Chiang HC, Choksi S, Liu J*, et al.* Plasma membrane translocation of trimerized MLKL protein is required for TNF-induced necroptosis. *Nature cell biology* 2014, **16**(1)**:** 55-65.

12. Chen X, Li W, Ren J, Huang D, He WT, Song Y*, et al.* Translocation of mixed lineage kinase domain-like protein to plasma membrane leads to necrotic cell death. *Cell research* 2014, **24**(1)**:** 105-121.

13. Dondelinger Y, Declercq W, Montessuit S, Roelandt R, Goncalves A, Bruggeman I*, et al.* MLKL compromises plasma membrane integrity by binding to phosphatidylinositol phosphates. *Cell reports* 2014, **7**(4)**:** 971-981.

14. Wang H, Sun L, Su L, Rizo J, Liu L, Wang LF*, et al.* Mixed Lineage Kinase Domain-like Protein MLKL Causes Necrotic Membrane Disruption upon Phosphorylation by RIP3. *Molecular cell* 2014, **54**(1)**:** 133-146.

15. Tanzer MC, Tripaydonis A, Webb AI, Young SN, Varghese LN, Hall C*, et al.* Necroptosis signalling is tuned by phosphorylation of MLKL residues outside the pseudokinase domain activation loop. *Biochemical Journal* 2015, **471**(2)**:** 255-265.

16. Linkermann A, Green DR. Necroptosis. *N Engl J Med* 2014, **370**(5)**:** 455-465.

17. Rodriguez DA, Weinlich R, Brown S, Guy C, Fitzgerald P, Dillon CP*, et al.* Characterization of RIPK3-mediated phosphorylation of the activation loop of MLKL during necroptosis. *Cell Death Differ* 2015, **In press**(doi: 10.1038/cdd.2015.70).

18. Su L, Quade B, Wang H, Sun L, Wang X, Rizo J. A plug release mechanism for membrane permeation by MLKL. *Structure* 2014, **22**(10)**:** 1489-1500.

19. Yoon S, Bogdanov K, Kovalenko A, Wallach D. Necroptosis is preceded by nuclear translocation of the signaling proteins that induce it. *Cell Death Differ* 2015, **In press**(doi: 10.1038/cdd.2015.92).

20. Tait SW, Oberst A, Quarato G, Milasta S, Haller M, Wang R*, et al.* Widespread mitochondrial depletion via mitophagy does not compromise necroptosis. *Cell reports* 2013, **5**(4)**:** 878-885.

21. Cook WD, Moujalled DM, Ralph TJ, Lock P, Young SN, Murphy JM*, et al.* RIPK1- and RIPK3-induced cell death mode is determined by target availability. *Cell Death Differ* 2014, **21**(10)**:** 1600-1612.

22. Chen W, Zhou Z, Li L, Zhong CQ, Zheng X, Wu X*, et al.* Diverse sequence determinants control human and mouse receptor interacting protein 3 (RIP3) and mixed lineage kinase domain-like (MLKL) interaction in necroptotic signaling. *J Biol Chem* 2013, **288**(23)**:** 16247-16261.

23. Jacobsen AV, Lowes KN, Tanzer MC, Lucet IS, Hildebrand JM, Petrie EJ*, et al.* HSP90 activity is required for MLKL oligomerisation and membrane translocation and the induction of necroptotic cell death. *Cell Death Dis*, **In press**.

24. Lawlor KE, Khan N, Mildenhall A, Gerlic M, Croker BA, D'Cruz AA*, et al.* RIPK3 promotes cell death and NLRP3 inflammasome activation in the absence of MLKL. *Nat Commun* 2015, **6:** 6282.

25. Murphy JM, Vince JE. Post-translational control of RIPK3 and MLKL mediated necroptotic cell death. *F1000Research* 2015, **4(F1000 Faculty Rev):** 1297.

26. Moujalled DM, Cook WD, Murphy JM, Vaux DL. Necroptosis induced by RIPK3 requires MLKL but not Drp1. *Cell Death Dis* 2014, **5:** e1086.

27. Remijsen Q, Goossens V, Grootjans S, Van den Haute C, Vanlangenakker N, Dondelinger Y*, et al.* Depletion of RIPK3 or MLKL blocks TNF-driven necroptosis and switches towards a delayed RIPK1 kinase-dependent apoptosis. *Cell Death Dis* 2014, **5:** e1004.

28. Schenk B, Fulda S. Reactive oxygen species regulate Smac mimetic/TNFalpha-induced necroptotic signaling and cell death. *Oncogene* 2015, **In press**(doi: 10.1038/onc.2015.35).

29. Murphy JM, Lucet IS, Hildebrand JM, Tanzer MC, Young SN, Sharma P*, et al.* Insights into the evolution of divergent nucleotide-binding mechanisms among pseudokinases revealed by crystal structures of human and mouse MLKL. *Biochemical Journal* 2014, **457**(3)**:** 369-377.

30. Murphy JM, Czabotar PE, Hildebrand JM, Lucet IS, Zhang JG, Alvarez-Diaz S*, et al.* The pseudokinase MLKL mediates necroptosis via a molecular switch mechanism. *Immunity* 2013, **39**(3)**:** 443-453.

31. Murphy JM, Zhang Q, Young SN, Reese ML, Bailey FP, Eyers PA*, et al.* A robust methodology to subclassify pseudokinases based on their nucleotide binding properties. *Biochemical Journal* 2014, **457**(2)**:** 323-334.

32. Fridriksson EK, Shipkova PA, Sheets ED, Holowka D, Baird B, McLafferty FW. Quantitative analysis of phospholipids in functionally important membrane domains from RBL-2H3 mast cells using tandem high-resolution mass spectrometry. *Biochemistry* 1999, **38**(25)**:** 8056-8063.

33. Xu C, Gagnon E, Call ME, Schnell JR, Schwieters CD, Carman CV*, et al.* Regulation of T cell receptor activation by dynamic membrane binding of the CD3epsilon cytoplasmic tyrosine-based motif. *Cell* 2008, **135**(4)**:** 702-713.

FIGURE LEGENDS

Figure 1: Human MLKL N-terminal domain and 4HB domain constructs require forced dimerisation to induce cell death in human cell lines.

(A-C) U937, HT29 and HeLa cells were stably infected with doxycycline inducible constructs encoding human MLKL (1-180). Expression was induced for 4 hours with 10 ng/ml doxycycline followed by induction of apoptosis (TS) or necroptosis (TSQ) or no treatment (untreated; UT) for 48 hours.

(D, E) Schematic representing coumermycin induced dimerisation of MLKL (1-180) (D) or MLKL 4HB domain (E) fused to gyrase.

(F-K) U937 (F, G), HT29 (H, I) and HeLa (J, K) cells were stably infected with doxycycline inducible constructs encoding human MLKL (1-180)-gyrase or human MLKL 4HB domain (1-125)-gyrase. Expression and dimerisation were induced for 4 hours with 10 ng/ml doxycycline and 700 nM coumermycin, followed by induction of apoptosis with TS or necroptosis with TSQ or no further treatment (UT) for 48 hours. Cell death was quantified by measuring PI-permeable cells using flow cytometry throughout. A statistical comparison of untreated, dox-induced conditions in the absence vs presence of coumermycin using a paired t-test yielded P-values of 0.081 and 0.0012 in Figures 1F and 1G, respectively.

All data are plotted as the mean ± SEM of at least three independent experiments.

Figure 2: Human and mouse N-terminal domain constructs or full-length phosphomimetic MLKL mutants rarely induce cell death in cells of the opposite species.

(A-D) Wild-type and *Mlkl*$^{-/-}$ mouse dermal fibroblasts (MDFs) were stably infected with doxycycline inducible constructs encoding human (1-180)-gyrase (A, B) or human 4HB domain (1-125)-gyrase (C, D). Expression and dimerisation were induced for 4 hours with 10

ng/ml doxycycline and 700 nM coumermycin, before induction of apoptosis (TS) or necroptosis (TSQ) or no treatment (UT) for 24 hours.

(E) *Mlkl*$^{-/-}$ MDFs were stably infected with doxycycline inducible constructs encoding human MLKL (1-471). After 4 hours of doxycycline (10 ng/ml) treatment to induce expression, cells were either stimulated for 24 hours with TS to induce apoptosis or TSQ to induce necroptosis or left untreated (UT).

Cell death was quantified by measuring PI-permeable cells using flow cytometry and data are plotted as the mean ± SEM of three biological replicates assayed in three independent experiments (n=9).

(F-K) Wild-type and *Mlkl*$^{-/-}$ MDFs, U937 and HT29 were stably infected with doxycycline inducible constructs encoding human full-length MLKL mutant (T357E/S358E), mouse full length MLKL mutant (S345D) and mouse MLKL (1-180), as indicated. After 4 hours of doxycycline (10 ng/ml) treatment to induce expression, cells were stimulated for 48 hours (U937, HT29) or 24 hours (MDFs) with TS to induce apoptosis or TSQ to induce necroptosis or left untreated (UT). Data are plotted as the mean ± SEM of at least three independent experiments for U937 and HT29 and of at least three biological replicates each assayed in a minimum of two independent experiments for MDFs. Cell death was quantified by measuring PI-permeable cells using flow cytometry throughout.

(L) Membrane complex (complex II) formation monitored by Blue-Native PAGE after a 14-hour induction of mouse full length MLKL S345D and human MLKL NTD (1-180) in U937 cells using 10 ng/ml doxycycline. Membrane fractionation purity and protein abundance was assessed by immunoblotting for GAPDH and VDAC. Data are representative of two independent repeats.

Figure 3: Gyrase mediated dimerisation of full-length mouse MLKL causes cell death, but is unable to overcome loss of function mutations in the 4HB domain.

(A) Schematic representing coumermycin induced dimerisation of full-length mouse MLKL fused to gyrase at the C-terminus.

(B) Cartoon of the 4HB domain showing the positions of loss of function mutations as sticks in blue (R105/D106) and red (E109/E110). Figure drawn using PyMol (www.pymol.org) from the co-ordinates of the full-length mouse MLKL structure (PDB accession, 4BTF; ref[5]).

(C, E, G) Wild-type and (D, F, H) *Mlkl*$^{-/-}$ MDFs were stably infected with doxycycline inducible constructs encoding for wild-type, E109A/E110A, R105A/D106A full-length mouse MLKL (1-464), as indicated. Expression and dimerisation were induced for 4 hours with 10 ng/ml doxycycline and 700 nM coumermycin, before induction of apoptosis (TS) or necroptosis (TSQ) or no treatment (UT) for 24 hours. Cell death was quantified by measuring PI-permeable cells using flow cytometry and data are plotted as the mean ± SEM of at least three biological replicates each assayed in a minimum of two independent experiments (n≥6).

Figure 4: Gyrase mediated dimerisation of full-length wild-type or T357E/S358E hMLKL is required for cell death.

Wild-type (A, B) and *Mlkl*$^{-/-}$ (C, D) MDFs, U937 (E, F), HT29 (G, H) and HeLa (I, J) were stably infected with doxycycline inducible constructs encoding C-terminal gyrase fusions of wild-type (left panels) or T357E/S358E (TSEE; right panels) human MLKL (1-471). Expression and dimerisation were induced for 4 hours with 10 ng/ml doxycycline and 700 nM coumermycin, before induction of apoptosis (TS) or necroptosis (TSQ) or no treatment (UT) for 24 hours for MDFs or 48 hours for human cell lines. Cell death was quantified by measuring PI-permeable cells using flow cytometry. Data are plotted as the mean ± SEM of at

least three independent experiments for U937 and HT29 and of at least three biological replicates each assayed in a minimum of two independent experiments for MDFs.

Figure 5: Mouse, horse and frog MLKL N-terminal domains kill mouse MDFs, but chicken and stickleback NTDs do not.

(A) Alignment of the 4HB domain amino acid sequences of MLKL orthologs. Numbering and schematic depiction of secondary structure shown above sequences corresponds to that of the mouse ortholog. Green shaded sequences are orthologous to R105 and E109 in mouse MLKL.

(B-G) Three biologically independent MDF cell lines derived from *Mlkl*$^{-/-}$ mice were stably infected with the indicated doxycycline-inducible NTD construct from different MLKL orthologs. Expression was induced for four hours with 10 ng/ml doxycycline before inducing apoptosis (TS) or necroptosis (TSQ) or no treatment (UT). Cell death was analysed in at least two independent experiments by detecting PI-permeable cells using flow cytometry. Data are plotted as the mean ± SEM (n≥6). Expression of these constructs was confirmed by Western blot in Supplementary Figure 2. In Figure 5E, a statistical comparison of uninduced vs dox-induced untreated cells using a paired t-test yielded a P-value of 0.0081.

(H) Separation of cytoplasmic and membrane fractions on Blue-Native PAGE after a 16 hour induction using 50 ng/ml doxycycline of mouse MLKL NTD (1-180) and horse MLKL NTD (1-189) C-terminally tagged with StrepII. Membrane fractionation purity and protein abundance was assessed by immunoblotting for GAPDH and VDAC. Data are representative of three independent repeats.

Figure 6: Plasma membrane permeabilization is an intrinsic property of MLKL NTDs.

(A) Schematic representation of the steps preceding membrane permeabilization downstream of full length MLKL activation following RIPK3-mediated phosphorylation (left panel) or expression of NTD constructs (right). The cellular data presented in Figures 1-5 suggest that other putative factors (X1, X2, X3 and X4) regulate MLKL activation (A), oligomerization (B), membrane translocation (C) and permeabilization (D), and that the brace helices can dampen 4HB domain-induced death in some cell lines. Recent work has implicated the co-chaperone system, Cdc37-HSP90, as one such factor that operates as a putative X1 on full length MLKL[23]. RIPK1 and RIPK3 are shown in brown and yellow, respectively; MLKL is depicted in orange; the putative regulators, X1-X4, are shown in blue.

(B) Left panel, recombinant mouse MLKL pseudokinase domain (179-464) and N-terminal domains of mouse (residues 1-169), human (2-154) and chicken (2-156) MLKL (~1 μg) were resolved by reducing SDS-PAGE and stained with Simply Blue Safe Stain (LifeTechnologies). Right panel, recombinant human (190-471) and frog (195-498) MLKL pseudokinase domains and full length human (2-471), chicken (2-486) and frog (2-498) MLKL (~1 μg) were similarly resolved and stained.

(C-K) Liposomes containing the self-quenching dye 5(6)-carboxyfluorescein were exposed to 1 μM recombinant protein as indicated and dye release was monitored spectrophotometrically over 3.25 hours. Data are plotted as the mean ± SD of 3-5 independent experiments, except for frog MLKL (2-498), which corresponds to mean ± SD of 2 independent experiments. Red data and curves represent plasma membrane composition liposomes while those in black signify mitochondrial like membranes.

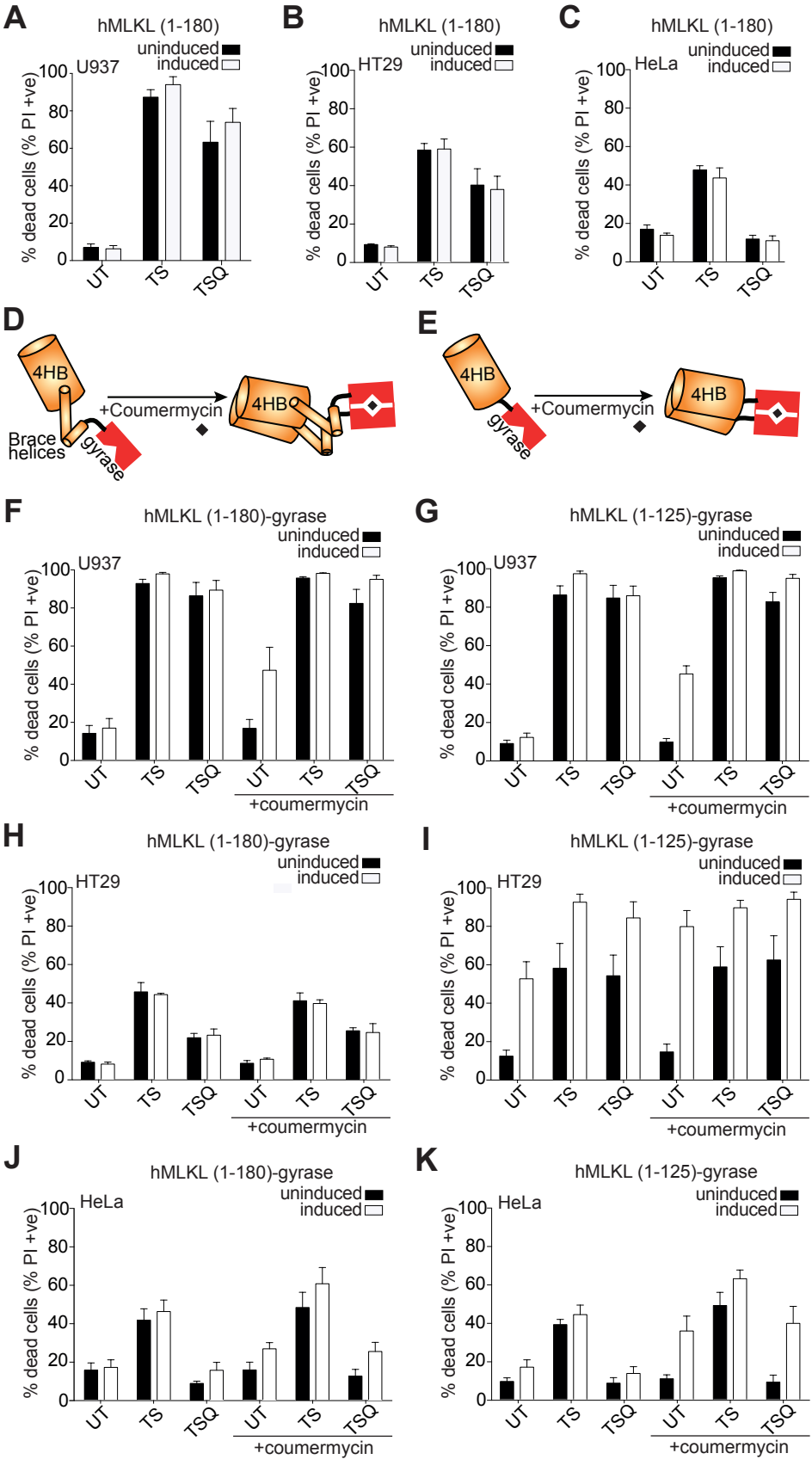
A
hMLKL (1-180)
U937
uninduced
induced
% dead cells (% PI +ve)
UT
TS
TSQ
B
hMLKL (1-180)
HT29
C
hMLKL (1-180)
HeLa
D
4HB
+Coumermycin
Brace helices
gyrase
E
F
hMLKL (1-180)-gyrase
+coumermycin
G
hMLKL (1-125)-gyrase
H
I
J
K

Figure 1

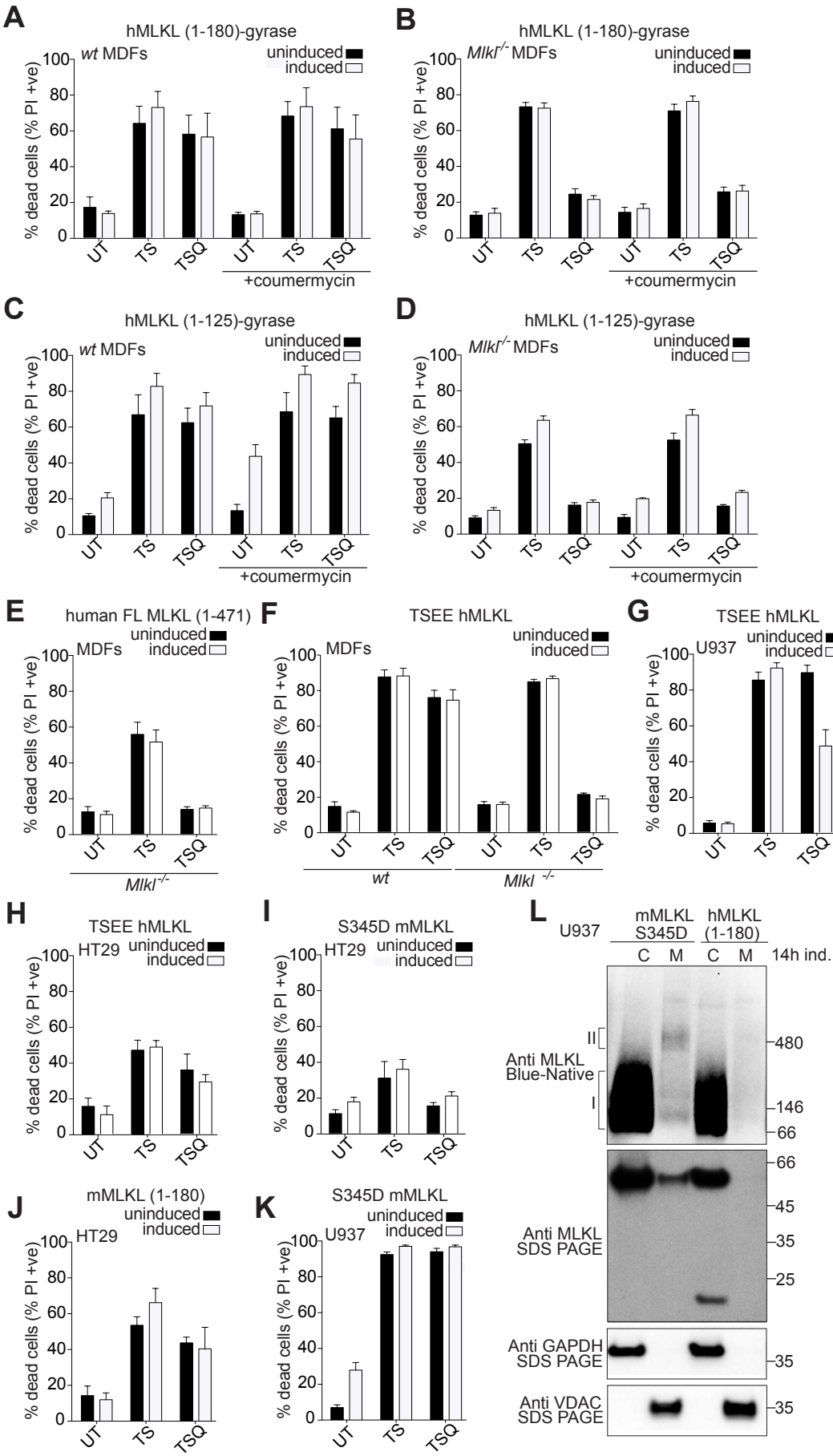
A
hMLKL (1-180)-gyrase
wt MDFs
uninduced
induced
% dead cells (% PI +ve)
UT
TS
TSQ
+coumermycin
B
hMLKL (1-180)-gyrase
Mlkl-/- MDFs
C
hMLKL (1-125)-gyrase
wt MDFs
D
hMLKL (1-125)-gyrase
Mlkl-/- MDFs
E
human FL MLKL (1-471)
MDFs
Mlkl-/-
F
TSEE hMLKL
MDFs
wt
Mlkl -/-
G
TSEE hMLKL
U937
H
TSEE hMLKL
HT29
I
S345D mMLKL
HT29
J
mMLKL (1-180)
HT29
K
S345D mMLKL
U937
L
U937
mMLKL S345D
hMLKL (1-180)
C
M
14h ind.
II
I
Anti MLKL Blue-Native
480
146
66
Anti MLKL SDS PAGE
45
35
25
Anti GAPDH SDS PAGE
Anti VDAC SDS PAGE

Figure 2

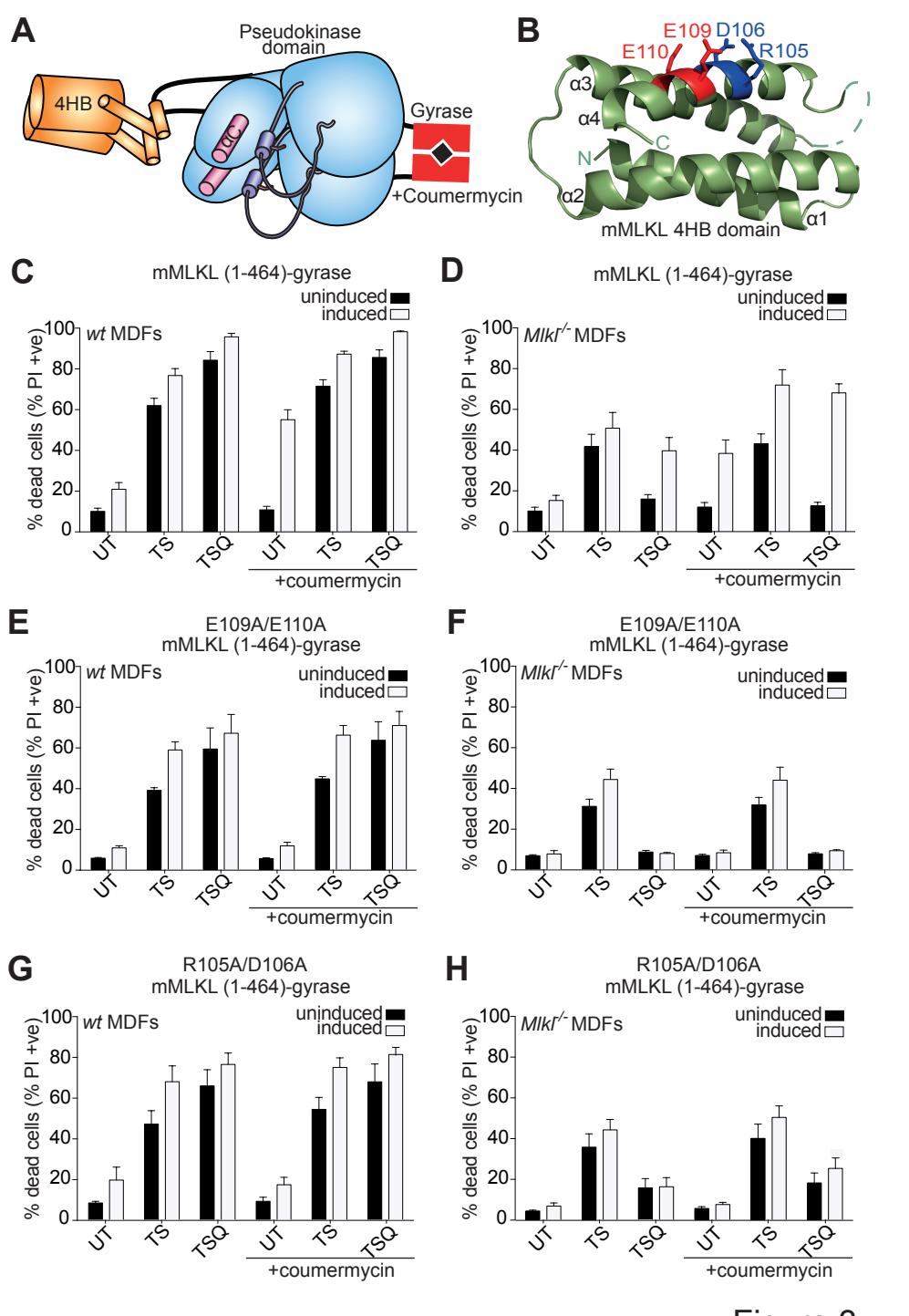
A
Pseudokinase domain
4HB
Gyrase
+Coumermycin
B
E109 D106
E110
R105
α3
α4
N
C
α2
α1
mMLKL 4HB domain
C
mMLKL (1-464)-gyrase
uninduced
induced
wt MDFs
% dead cells (% PI +ve)
UT
TS
TSQ
+coumermycin
D
mMLKL (1-464)-gyrase
Mlkl-/- MDFs
E
E109A/E110A
mMLKL (1-464)-gyrase
wt MDFs
F
E109A/E110A
mMLKL (1-464)-gyrase
Mlkl-/- MDFs
G
R105A/D106A
mMLKL (1-464)-gyrase
wt MDFs
H
R105A/D106A
mMLKL (1-464)-gyrase
Mlkl-/- MDFs

Figure 3

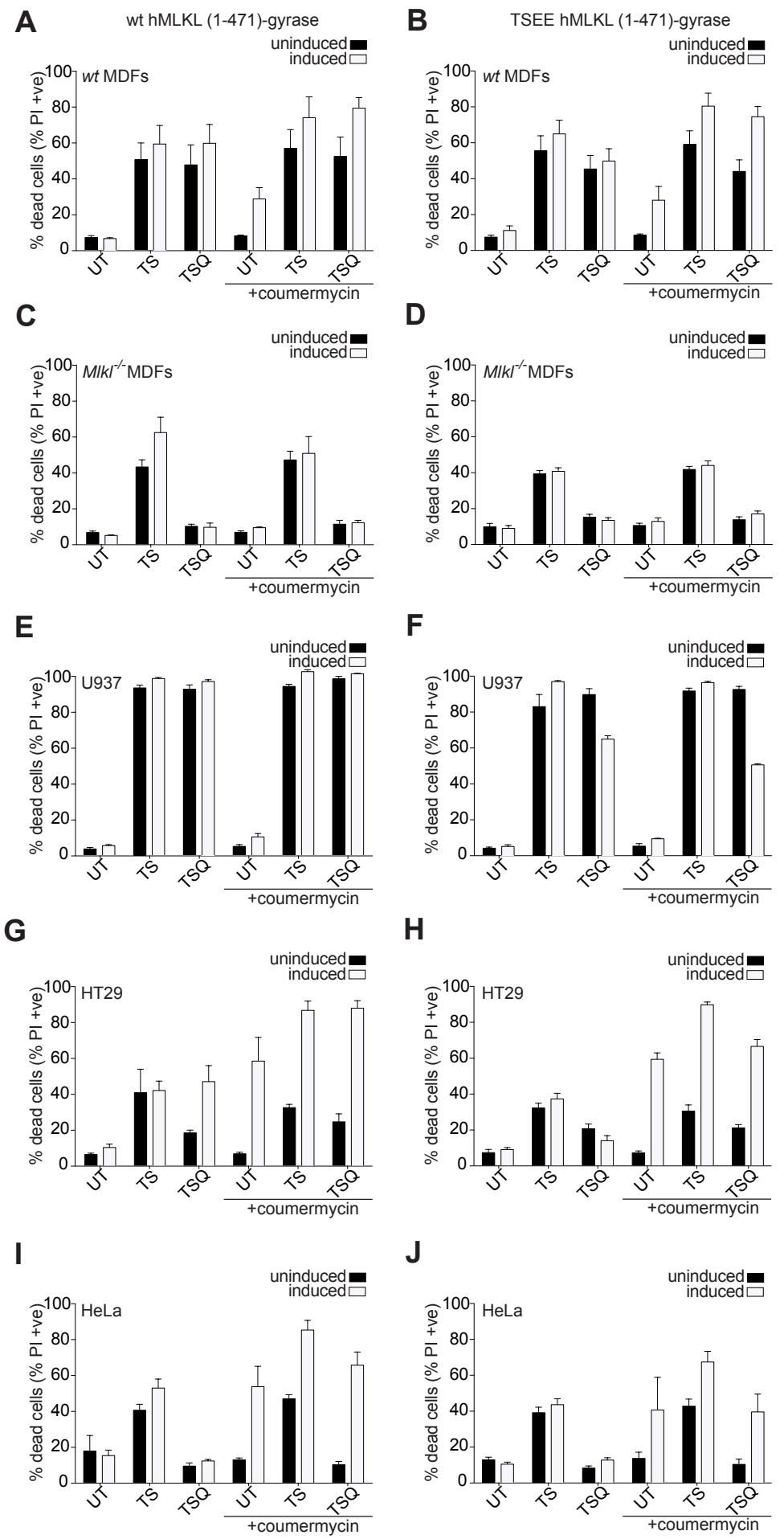
A
wt hMLKL (1-471)-gyrase
uninduced
induced
wt MDFs
% dead cells (% PI +ve)
UT
TS
TSQ
+coumermycin
B
TSEE hMLKL (1-471)-gyrase
C
Mlkl-/- MDFs
D
E
U937
F
G
HT29
H
I
HeLa
J

Fig. 4

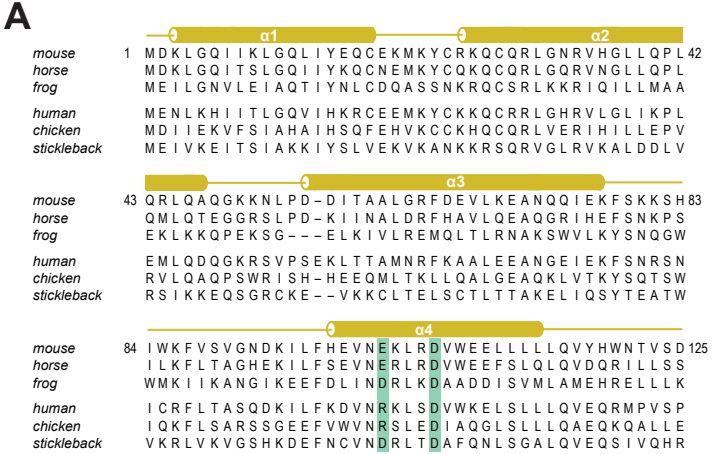
A
α1
α2
α3
α4
mouse 1 MDKLGQIIKLGQLIYEQCEKMKYCRKQCQRLGNRVHGLLQPL 42
horse MDKLGQITSLGQIIYKQCNEMKYCQKQCQRLGQRVNGLLQPL
frog MEILGNVLEIAQTIYNLCDQASSNKRQCSRLKKRIQILLMAA
human MENLKHIITLGQVIHKRCEEMKYCKKQCRRLGHRVLGLIKPL
chicken MDIIEKVFSIAHAIHSQFEHVKCCKHQCQRLVERIHILLEPV
stickleback MEIVKEITSIAKKIYSLVEKVKANKKRSQRVGLRVKALDDLV
mouse 43 QRLQAQGKKNLPD-DITAALGRFDEVLKEANQQIEKFSKKSH 83
horse QMLQTEGGRSLPD-KIINALDRFHAVLQEAQGRIHEFSNKPS
frog EKLKKQPEKSG---ELKIVLREMQLTLRNAKSWVLKYSNQGW
human EMLQDQGKRSVPSEKLTTAMNRFKAALEEANGEIEKFSNRSN
chicken RVLQAQPSWRISH-HEEQMLTKLLQALGEAQKLVTKYSQTSW
stickleback RSIKKEQSGRCKE--VKKCLTELSCTLTTAKELIQSYTEATW
mouse 84 IWKFVSVGNDKILFHEVNEKLRDVWEELLLLLQVYHWNTVSD 125
horse ILKFLTAGHEKILFSEVNERLRDVWEEFSLQLQVDQRILLSS
frog WMKIIKANGIKEEFDLINDRLKDAADDISVMLAMEHRELLLK
human ICRFLTASQDKILFKDVNRKLSDVWKELSLLLQVEQRMPVSP
chicken IQKFLSARSSGEEFVWVNRSLEDIAQGLSLLLQAEQKQALLE
stickleback VKRLVKVGSHKDEFNCVNDRLTDAFQNLSGALQVEQSIVQHR
H
mouse (1-180)
horse MLKL (1-189)
C M C M 16h ind.
II
I
Anti MLKL Blue-Native
480
146
66
Anti MLKL SDS PAGE
66
45
Anti GAPDH SDS PAGE
35
Anti VDAC SDS PAGE
35

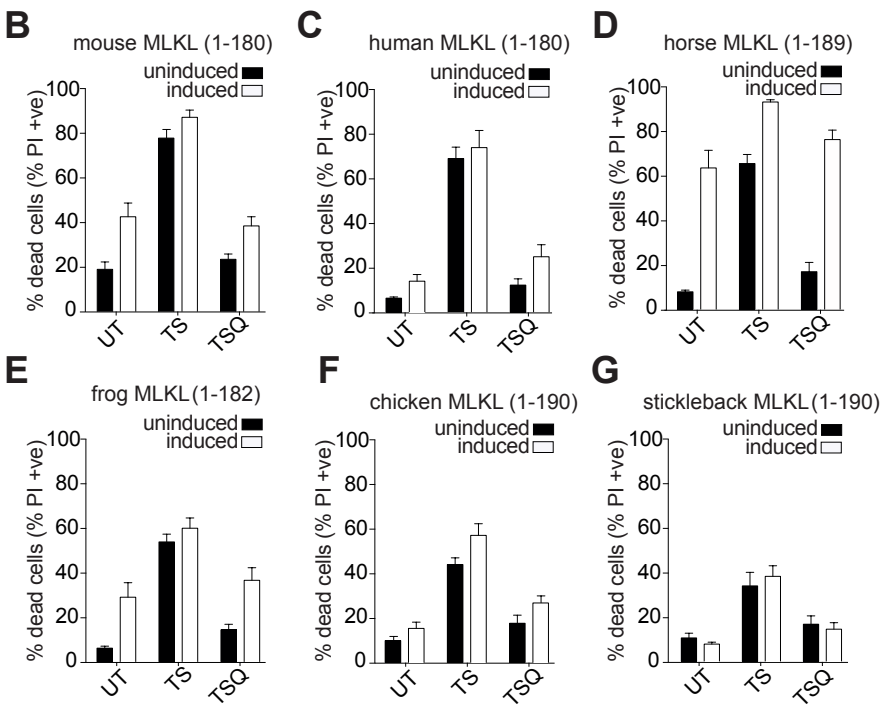
B
mouse MLKL (1-180)
C
human MLKL (1-180)
D
horse MLKL (1-189)
E
frog MLKL (1-182)
F
chicken MLKL (1-190)
G
stickleback MLKL (1-190)
uninduced
induced
% dead cells (% PI +ve)
0
20
40
60
80
100
UT
TS
TSQ

Figure 5

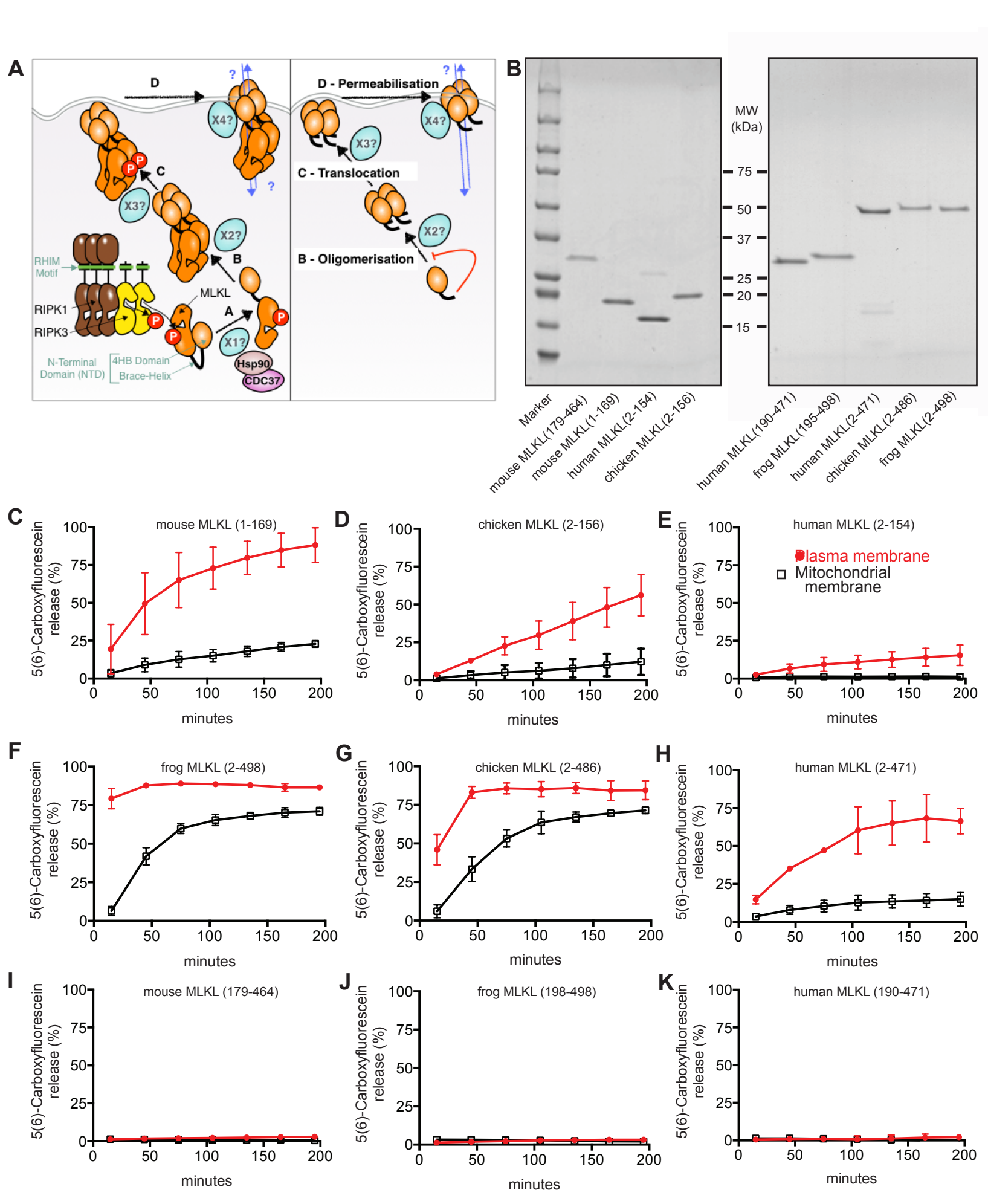
A
D
D - Permeabilisation
C
C - Translocation
B
B - Oligomerisation
A
MLKL
RIPK1
RIPK3
RHIM Motif
N-Terminal Domain (NTD)
4HB Domain
Brace-Helix
Hsp90
CDC37
X1?
X2?
X3?
X4?
B
MW (kDa)
75
50
37
25
20
15
Marker
mouse MLKL(179-464)
mouse MLKL(1-169)
human MLKL(2-154)
chicken MLKL(2-156)
human MLKL(190-471)
frog MLKL(195-498)
human MLKL(2-471)
chicken MLKL(2-486)
frog MLKL(2-498)
C
mouse MLKL (1-169)
D
chicken MLKL (2-156)
E
human MLKL (2-154)
Plasma membrane
Mitochondrial membrane
F
frog MLKL (2-498)
G
chicken MLKL (2-486)
H
human MLKL (2-471)
I
mouse MLKL (179-464)
J
frog MLKL (198-498)
K
human MLKL (190-471)
5(6)-Carboxyfluorescein release (%)
minutes
0
25
50
75
100
150
200

Figure 6